

# Evaporation Rate and Equilibrium Phase Separation Data in Relation to Casting Conditions and Performance of Porous Cellulose Acetate Reverse Osmosis Membranes

B. KUNST\* and S. SOURIRAJAN, *Division of Chemistry, National  
Research Council of Canada, Ottawa, Canada*

## Synopsis

Quantitative data on solvent evaporation rates and equilibrium phase separation compositions corresponding to different film casting conditions are given, and the results are discussed with reference to reverse osmosis data on membrane performance. A typical evaporation rate curve plotted on a semilog scale consists of an initial linear part from whose slope evaporation rate constants  $b$  have been determined. For a given casting solution composition and temperature, an optimum value of  $b$  exists for best membrane performance, and identical values of  $b$  result in same membrane performance. Treating the casting solution as a polymer-solvent-nonsolvent ternary system, the data on equilibrium phase separation compositions have been plotted in a triangular diagram for solution temperatures of  $-10^\circ$ ,  $0^\circ$ , and  $24^\circ\text{C}$ . The data indicate that even small changes in solution temperature can bring about significant changes in solution structure and hence membrane performance, and useful conclusions on solution structure can be drawn from such phase equilibrium diagrams. The data and correlations presented here offer a quantitative confirmation of the governing significance of the solution structure-evaporation rate concept relating to the mechanism of phase separation and pore formation in the surface region during the process of making reverse osmosis membranes.

## INTRODUCTION

The mechanism of phase separation and pore formation in the process of making the Loeb-Sourirajan-type cellulose acetate membranes and the effect of casting conditions on the performance of such membranes in reverse osmosis experiments have been discussed.<sup>1</sup> The experimental results presented led to a new approach to the general problem of developing more productive reverse osmosis membranes.<sup>1,2</sup> In this approach, the composition and temperature of the casting solution (solution structure) and the solvent evaporation rate during film formation together constitute an important interconnected variable governing the surface pore structure, and hence the performance, of the resulting membranes in reverse osmosis.

\* Present address: Institute of Physical Chemistry, Faculty of Technology, University of Zagreb, Zagreb, Yugoslavia.

The object of this paper is to present the relevant quantitative data on solvent evaporation rates and equilibrium phase separation conditions in the surface region and discuss such data with reference to those on membrane performance reported earlier.<sup>1</sup>

The different steps involved in the membrane-making procedure have been listed and discussed;<sup>1</sup> all details relating to each one of these steps are obviously important with respect to the overall porous structure of the resulting membranes. This paper, however, is concerned only with the changes taking place in the surface region of the membrane during film formation, and all references to pores refer to those in the surface region.

## EXPERIMENTAL

### Solvent Evaporation Rate Measurements

These were made by determining the weight change of the polymer film cast on a small glass plate as a function of time.

The measurements all refer to the same following casting solution composition: acetone, 68.0 wt-%; cellulose acetate (acetyl content = 39.8%), 17.0 wt-%; water, 13.5 wt-% and magnesium perchlorate 1.5 wt-%. This composition is the same as that used earlier<sup>1</sup> for the CA-NRC-18 (or simply, Batch 18)-type films. Different solution temperatures and evaporation conditions were maintained during film casting for which small glass plates ( $\sim 17$  mm  $\times$  38 mm), with side runners to give the required film thickness, were used. Unless otherwise noted, the thickness of the side runner was the same as that generally used in making films for reverse osmosis experiments. The polymer solution and the glass plates were always kept at the required solution temperature for at least 24 hr prior to casting.

The evaporation rate measurements were carried out at constant temperature of surroundings either in a cold room or in the laboratory, as required. The polymer solution was spread on the glass plate by moving an inclined knife on the side runners and immediately transferred to an analytical balance. As the acetone evaporated, the weight (in grams) of the plate containing the film decreased, and this change in weight was followed as a function of time. The first weight was noted 30 sec after casting, and the subsequent weights were noted in 15-sec intervals for a few minutes; the weight at any time,  $t$ , was designated as  $W_t$ . As the changes in weight became less, the weights were noted after longer time intervals, until essentially constant weight,  $W_\infty$ , was reached. The weight determinations were continued for about 1 hr even though the change in weight became progressively insignificant after the first 10 min.

Several such measurements were also made while solvent evaporation took place in an atmosphere of acetone vapor. Prior to those measurements, the closed space of the analytical balance was kept in contact with the required concentration of aqueous acetone solution placed in several shallow open containers for 1 to 2 hr.

### Determination of Equilibrium Phase Separation Data

For the purpose of this determination, the casting solution was treated as a ternary system consisting of polymer (cellulose acetate), solvent (acetone), and nonsolvent (magnesium perchlorate to water ratio, 1:9). All compositions stated are in weight per cent. Stock solutions of different concentrations of cellulose acetate in acetone ( $\sim 10, 15, 20, 22,$  and  $25$  wt-% polymer) were prepared. Several samples of each one of these solutions were accurately weighed in glass-stoppered flasks. To each one of these flasks a calculated quantity of the nonsolvent was added so that different compositions of the ternary system were obtained with successively increasing quantities of the nonsolvent-solvent ratio. Each flask was stirred at room temperature for one to six days to effect the maximum possible mixing of the components of the system. The ternary mixtures gave clear solutions at low values of nonsolvent-solvent ratio, but the solutions became more and more turbid at higher values of the above ratio due to polymer precipitation. By successively narrowing down the concentration range of the ternary system with respect to nonsolvent-solvent ratio, the boundary composition corresponding to the phase separation of the polymer was established. By repetition of such experiments at different temperatures for different values of polymer concentrations, the boundary curves, representing phase separation of the polymer in the ternary system, were obtained as given in the triangular composition diagram (Fig. 7).

At higher concentrations of the polymer solution, the nonsolvent-solvent ratio was varied essentially along lines of constant nonsolvent content in the ternary system. In all cases, the turbidity caused by phase separation of the polymer was recognized by visual observation.

In view of the uncertainties inherent in the visual method of establishing the turbidity of the system, no high degree of accuracy is claimed for the phase boundary lines presented in Figure 7. More sensitive experimental techniques of locating the phase separation compositions are clearly called for. However, visual techniques have been used before effectively.<sup>3</sup> Further, the method used here presented no difficulties at polymer concentrations of  $20$  wt-% or less; the data given in this concentration range are considered reasonably accurate for practical purposes. At higher polymer concentrations, the boundary compositions could not be fixed exactly; in that region, the indicated locations of the boundary lines are less precise.

### Reverse Osmosis Experiments

The method of making membranes and the details of experimental procedure used were the same as those reported earlier.<sup>1</sup>

## RESULTS AND DISCUSSION

### Evaporation Rate Data

The general trend of the rapid decrease in solvent loss with time is expressed by the evaporation rate measurements, which can conveniently be

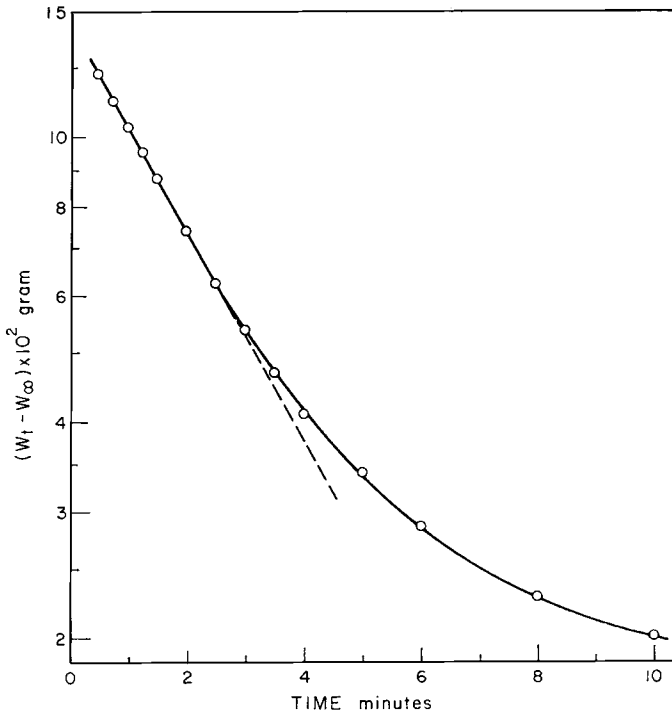


Fig. 1. A typical evaporation rate curve: Temperature of casting solution,  $0^\circ\text{C}$ ; casting atmosphere, ambient air at  $24^\circ\text{C}$ ; area of evaporation surface,  $\sim 6\text{ cm}^2$ .

represented by plotting the values of  $\log (W_t - W_\infty)$  in grams versus  $t$  in minutes. A typical set of such data is plotted in Figure 1, which shows that the evaporation rate curve so represented consists of an initial linear part followed by a nonlinear part. Both parts of the curve are obviously important to an understanding of the contribution of evaporation rate to the ultimate porous structure of the surface layer of the membrane.

The linear part of the curve probably indicates the constancy of the mechanism governing evaporation rate in the early stages of the process when it may be expected that the solvent loss from film surface is compensated by solvent diffusion to the film surface from underneath. In any case, since the cloud point (polymer phase separation) in the surface region may be expected to be reached soon after evaporation starts, the initial part of the curve is all important in representing the development of the formation of the porous structure of the surface region. Because the curve is linear in this part, it is also precisely defined.

Preliminary results showed that, for a given casting solution composition and temperature, the relative position and slope of the linear part of the curve depended not only on evaporation conditions (temperature and acetone content of the casting atmosphere) but also on the thickness and surface area  $S$  of the film. This is illustrated in Figure 2, where curves  $a$ ,  $b$ ,

and  $c$  represent the data for films of three different thicknesses and essentially the same surface area, and curves  $b$ ,  $d$  and  $e$  represent the data for films of three different areas but essentially the same film thickness (same as that used in making films for reverse osmosis experiments). A change in film thickness changes both the slope and relative position of the evaporation rate curve, whereas a change in surface area changes only the position but not the slope of the curve. Extrapolating the  $W_t - W_\infty$  versus  $t$  curve to zero time, the initial weight  $W_0$  of the plate containing the film could be determined, and the value of  $(W_0 - W_\infty)/S$ , representing the total quantity of solvent evaporated per unit area of film surface, could be calculated.

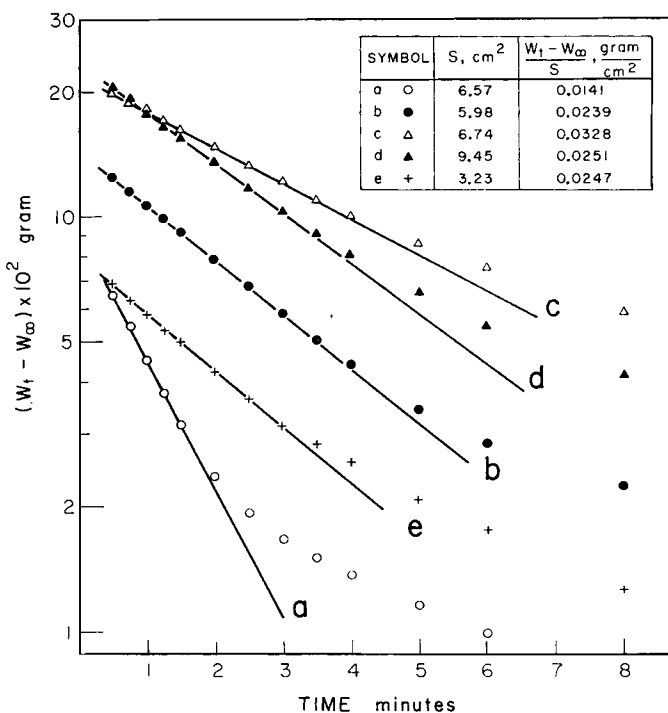


Fig. 2. Effect of film area and film thickness on evaporation rates: Temperature of casting solution, 0°C; casting atmosphere, ambient air at 24°C.

This quantity increases with increase in film thickness and remains essentially constant for constant film thickness with respect to the given casting solution composition. In all work on evaporation rate measurements reported and discussed in the rest of this paper, the area of the film surface was maintained constant at about 6 cm<sup>2</sup>, and the influence of variation of film thickness was eliminated by considering only those data for which  $(W_0 - W_\infty)/S$  was essentially constant, corresponding to the same film thickness as that normally used in making films for reverse osmosis experiments.

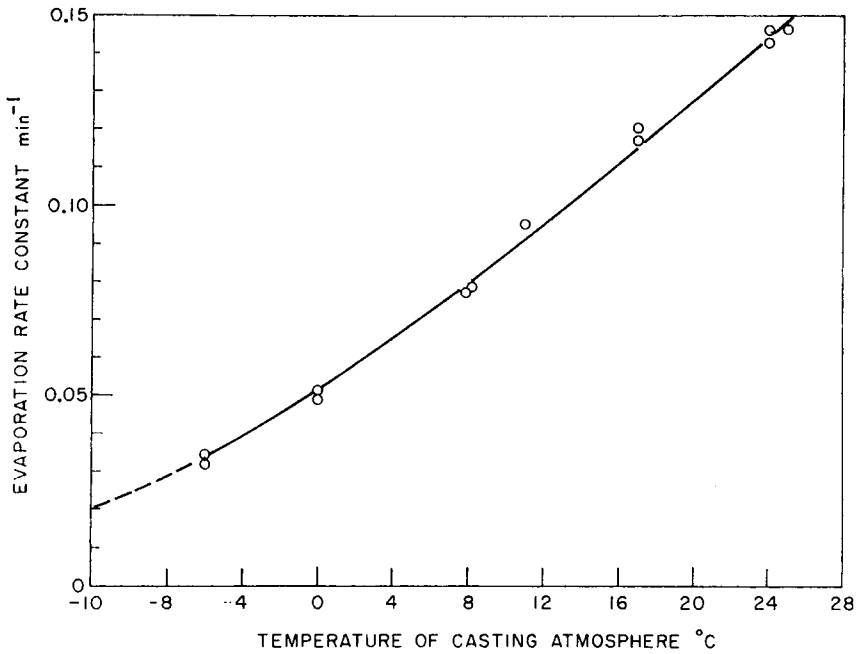


Fig. 3. Effect of temperature of casting atmosphere on evaporation rate: Temperature of casting solution, 0°C; casting atmosphere, ambient air.

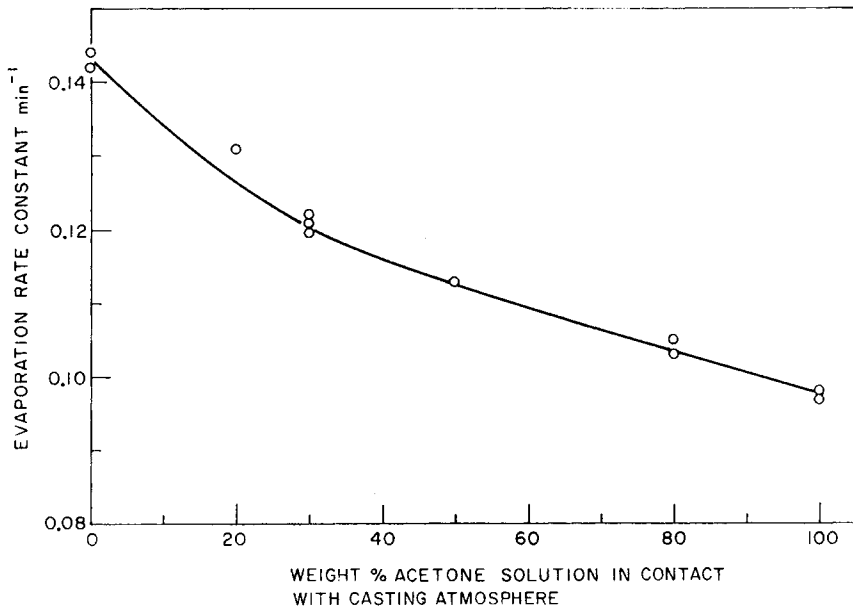


Fig. 4. Effect of presence of acetone vapor in casting atmosphere on evaporation rate: Temperature of casting solution, 0°C; temperature of casting atmosphere, 24°C.

For a given area of film surface, the linear part of the evaporation rate curve (Fig. 1) may be represented by the relation

$$W_t - W_\infty = (W_0 - W_\infty) e^{-bt},$$

where  $b$  is a constant which may appropriately be called the evaporation rate constant (in  $\text{min}^{-1}$ ). The factors affecting values of  $b$  and the specific values of  $b$  obtained under different film casting conditions are of practical interest.

Figure 3 gives the effect of temperature of the casting atmosphere on the value of  $b$  for the casting condition where the temperature of the casting solution was  $0^\circ\text{C}$  and the casting atmosphere was ambient air. The data show that  $b$  increases, almost linearly, with increase in temperature of the casting atmosphere. Figure 4 gives the effect of the presence of acetone in the casting atmosphere on the value of  $b$ ; these data correspond to the condition where the temperature of the casting solution was again  $0^\circ\text{C}$  and the temperature of the casting atmosphere was that of the ambient laboratory condition ( $24^\circ\text{C}$ ). These data show that the presence of acetone in the casting atmosphere reduces the value of  $b$ , and this reduction becomes progressively less steep with increasing saturation of the casting atmosphere with acetone. Thus, the introduction of acetone in the casting atmosphere offers a sensitive means of reducing  $b$ , which introduction can be appropriately combined with controlled temperature variation of the casting atmosphere itself to suit particular needs. The data given in Table I show that

TABLE I  
Effect of Casting Solution Temperature on  
Evaporation Rate Constant<sup>a</sup>

Temp of casting solution, $^\circ\text{C}$	Evaporation rate constant $b$ , $\text{min}^{-1}$
-10	0.133
0	0.145
24	0.167

<sup>a</sup> Casting solution composition: same as that for Batch 18 membranes; temperature of casting atmosphere:  $24^\circ\text{C}$ ; casting atmosphere: ambient air.

the temperature of the casting solution also affects  $b$  even though the conditions of the casting atmosphere are the same; the higher the solution temperature, the higher was the value of  $b$ . These data are particularly interesting because they illustrate that the evaporation rate is a function not only of the conditions of the casting atmosphere but also of those of the casting solution. The data presented in Figures 3 and 4, and Table I, give a quantitative confirmation of the statements made earlier<sup>1</sup> on the factors affecting evaporation rates during film formation.

Membrane performance data corresponding to seven different casting conditions were reported earlier.<sup>1</sup> The values of  $b$  corresponding to those casting conditions are given in Table II, which also gives the productivity of the respective films for the 90% level of solute separation in reverse

TABLE II  
Evaporation Rate Constants and Membrane Productivities  
Under Different Casting Conditions<sup>a</sup>

No. <sup>b</sup>	Casting conditions			Evaporation rate constant <i>b</i> , min <sup>-1</sup>	Membrane productivity at 90% solute sepn, <sup>c</sup> gal/day/ft <sup>2</sup>
	Temp of casting solution, °C	Temp of casting atm, °C	Casting atm in contact with acetone soln, wt %		
1	-10	-10	0	0.030	9.3
2	-10	-10	30	0.030	9.3
3	-10	0	0	0.051	9.3
4	0	0	30	0.048	12.3
5	0	24	0	0.145	17.6
6	0	24	30	0.121	19.4
7	0	24	80	0.104	21.0

<sup>a</sup> Casting solution composition: same as that for Batch 18 membranes.

<sup>b</sup> These numbers refer to those given in Figure 3 in our previous report.<sup>1</sup>

<sup>c</sup> Feed: 3500 ppm NaCl-H<sub>2</sub>O; operating pressure: 250 psig; mass transfer coefficient on high pressure side of membrane:  $45 \times 10^{-4}$  cm/sec.

osmosis experiments at 250 psig using 3500 ppm NaCl-H<sub>2</sub>O feed solutions and a mass transfer coefficient of  $45 \times 10^{-4}$  cm/sec. The numbers 1 to 7 given in the first column in Table II refer to casting conditions corresponding to performance curves 1 to 7 in Figure 3 of the previous paper.<sup>1</sup> The data on evaporation rate constants given in the last column of Table II confirm the statements made earlier<sup>1</sup> regarding possible changes in solvent evaporation rates at the respective casting conditions studied. Two further observations can be made. The values of *b* are the same for the casting conditions 1 and 2; this means that contacting the casting atmosphere with 30% acetone solution at -10°C did not change the evaporation rate significantly, probably because of the very low partial pressure of acetone vapor in the atmosphere under the casting conditions. Referring to casting conditions 4 to 7, the best membrane performance (data for condition 7) was obtained neither at the highest nor at the lowest value of *b*, which points out the existence of an optimum evaporation rate for a given casting solution structure from the point of view of best membrane performance. These observations further illustrate the validity of the concept that solution structure and evaporation rate together constitute an interconnected variable governing the ultimate porous structure of the surface layer of reverse osmosis membranes.

The significance of evaporation rate as a controlling parameter in the development of the porous structure of the membrane surface may be brought out by yet another consideration. The casting condition represented by No. 6 in Table II is taken here for illustration. The film obtained under these casting conditions using an evaporation period of 2 min are designated here as Batch 301 membranes, following the earlier nomenclature.<sup>2</sup> Referring to Figure 4, the value of *b* equals 0.12 min<sup>-1</sup>, corre-



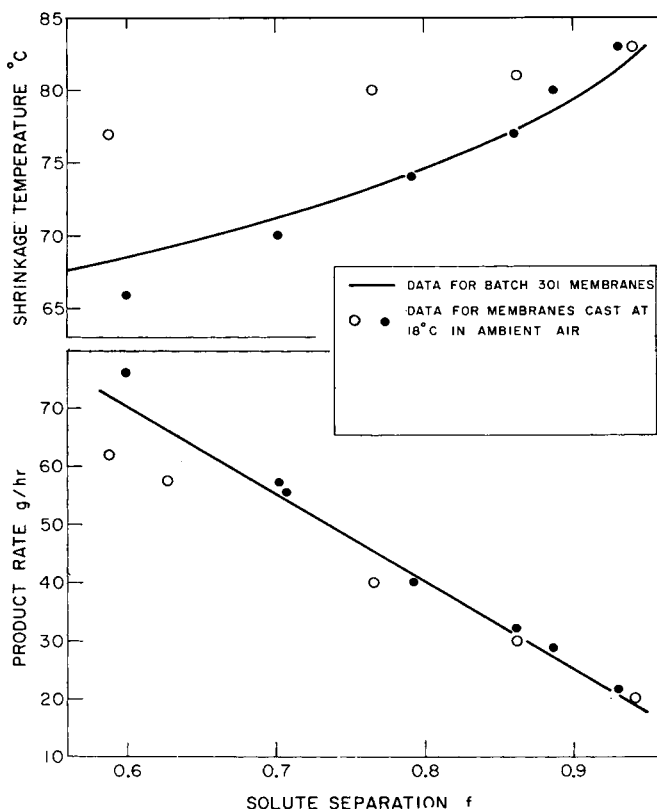


Fig. 5. Comparison of data on membrane performance and shrinkage temperature profile for films cast at 18°C in ambient air atmosphere with those of Batch 301 membranes: Temperature of casting solution, 0°C. Reverse osmosis data for conditions: feed, 3500 ppm NaCl-H<sub>2</sub>O; operating pressure, 250 psig; mass transfer coefficient,  $45 \times 10^{-4}$  cm/sec; membrane area, 7.6 cm<sup>2</sup>. Evaporation period: (O) 2 min; (●) 1 min.

sponding to casting atmosphere at 24°C in contact with an aqueous solution of 30% acetone; referring to Figure 3, the same value of  $b$  is obtained at 18°C ambient air casting atmosphere without any acetone. These two casting conditions are hence equivalent. Consequently, using a casting solution temperature of 0°C, membranes cast in acetone-free ambient air at 18°C may be expected to yield the same performance curve (solute separation-product rate correlation) as that given by the Batch 301 membranes. That this is indeed the case is illustrated by the experimental reverse osmosis data given in Figure 5.

The solid lines in the lower and upper part of Figure 5 represent, respectively, the performance data and the shrinkage temperature profile for the Batch 301 membranes; these lines are the same as those given earlier. For comparison, two sets of data (corresponding to evaporation periods of 2 min and 1 min, respectively) for films cast at 18°C ambient air atmosphere

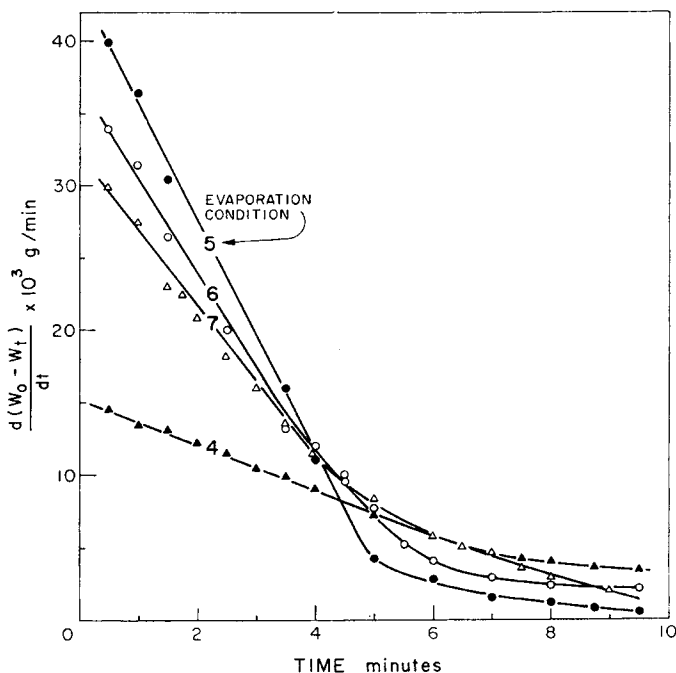


Fig. 6. Variation of solvent evaporation rate with time for different evaporation conditions specified in Table II.

without any acetone are also plotted in Figure 5. The results illustrate that, using casting solutions of identical structure, evaporation conditions during film casting corresponding to same values of  $b$  result in essentially equal membrane performance. This observation is of fundamental significance in reverse osmosis membrane science.

It has been shown that the shrinkage temperature profile is a function of evaporation time, and it does not affect the solute separation-product rate correlation (performance curve) for Batch 18-type films, which contain comparatively big and uniform surface pores.<sup>1</sup> Batch 301 films, however, contain smaller and less uniform pores; for these films, it is only reasonable to expect that a shift in the shrinkage temperature profile (which expresses pore size distribution) will also shift the membrane performance curve. Consequently, reproducibility of the performance of Batch 301 membranes should also depend on reproducing their shrinkage temperature profile. This is also indicated by the data plotted in Figure 5. Referring to data on shrinkage temperature profile with the membranes cast at 18°C, those obtained with a 1-min evaporation period are far closer to the corresponding profile of Batch 301 membranes than those obtained with a 2-min evaporation period. In all the three cases, films whose shrinkage temperature profile data are not too far separated exhibit essentially identical membrane performance. This observation is again one of fundamental significance

from the point of view of quality control in making reverse osmosis membranes.

No extensive interpretation of the nonlinear part of the evaporation rate curve is possible at this time for two reasons. In this region, the mechanism of solvent evaporation is complicated by several factors which are not precisely known; further, all the membranes for which performance data are available<sup>1,2</sup> were made with evaporation periods that were still in the linear part of the respective evaporation rate curves. However, it may be pertinent to call attention to Figure 6, which gives a plot of  $(d/dt)(W_0 - W_t)$  versus  $t$  expressing solvent evaporation rate as a function of time for four different evaporation conditions represented by the numbers 4 to 7 in Table II. Figure 6 shows that the evaporation rate curve so expressed may be considered as made up of essentially two linear parts indicating two dominating factors relating to the respective mechanisms of solvent evaporation. Further, it is seen that for all the four evaporation conditions studied, the  $(d/dt)(W_0 - W_t)$  versus  $t$  plot seems to converge essentially in a narrow time interval of about 4 to 5 min. It would be interesting to examine the corresponding performance and shrinkage temperature profile data with films made using different evaporation periods and see whether such convergence of evaporation rate data has any practical significance.

#### Equilibrium Phase Separation Data

The compositions at which phase separation occurs in the surface region with respect to the specified ternary polymer(P)–solvent(S)–nonsolvent(N) system at  $-10^\circ$ ,  $0^\circ$ , and  $24^\circ\text{C}$  are plotted in a triangular diagram in Figure 7, where the point *A* represents the composition of the casting solution used (P:S:N = 17:68:15) in making membranes for reverse osmosis studies. The point *A* is most remote from the phase boundary curve corresponding to the highest temperature. Using the casting solution represented by the point *A*, Figure 7 shows that the composition of the surface region will change along the line *AE* during solvent evaporation, and phase separation in the surface region will occur at compositions corresponding to points *B*, *C*, and *D* at solution temperatures of  $-10^\circ$ ,  $0^\circ$ , and  $24^\circ\text{C}$ , respectively.

It has been shown by Klenin and co-workers<sup>4,5</sup> that concentrated cellulose acetate solutions give rise to supermolecular polymer aggregates whose sizes decrease very sharply with increase in temperature. Consequently, one may conclude that the average size of the supermolecular aggregates in the polymer solution represented by point *A* decreases rapidly as the solution temperature increases from  $-10^\circ$  to  $24^\circ\text{C}$ .

The points *B* and *C* refer to solution temperatures of  $-10^\circ$  and  $0^\circ\text{C}$ , respectively; the membrane performance corresponding to the above solution temperatures is given by group I and group II curves in Figure 3 in our earlier report.<sup>1</sup> The results show that smaller size of supermolecular polymer aggregation gives rise to better membrane performance. Further, even though points *B* and *C* are not too far separated from each other, the group I and group II curves are significantly separated from each other.

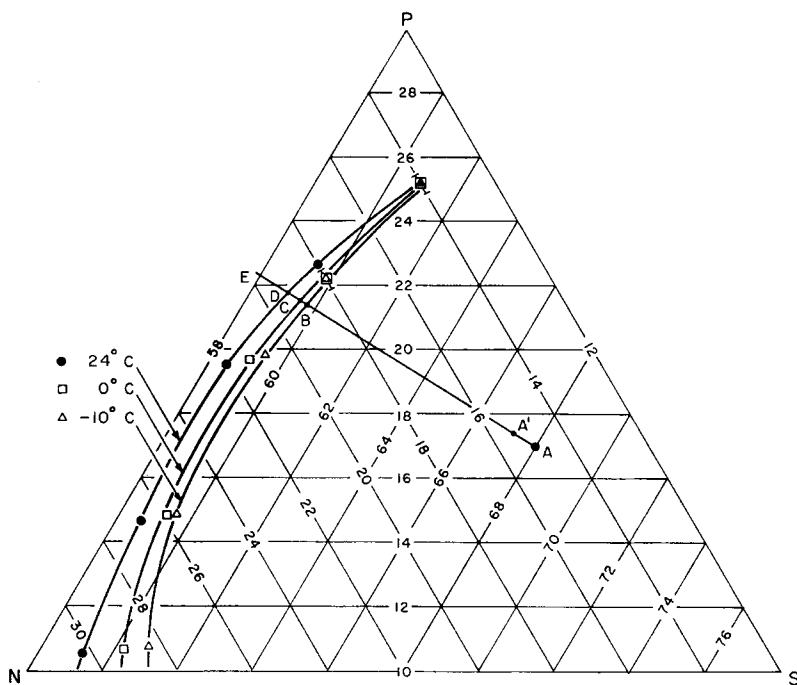


Fig. 7. Equilibrium phase separation compositions (weight-%) at different solution temperatures for the ternary system P(cellulose acetate)-S(acetone)-N(1:9 magnesium perchlorate-water).

This shows that even small changes in solution temperature will bring about significant changes in supermolecular aggregation and hence membrane performance.

Figure 7 also shows that compositions corresponding to points *B*, *C*, and *D* are different as a consequence of solvent evaporation; in particular, the polymer concentration at the phase boundary is slightly higher for higher solution temperatures. Further, the solvent evaporation process itself may tend to decrease the solution temperature slightly. These factors may also contribute to changes in the surface porous structure of membranes cast from solutions of different temperatures.

A set of new membranes was made using a casting solution composition of P:S:N = 17.4:67.2:15.4 represented by the point *A'* on line *AE* in Figure 7. These membranes were made using a casting solution temperature of 24°C; the casting conditions used were exactly the same as those given for Batch 301 membranes (casting condition 6, Table II). A set of reverse osmosis experiments was carried out with the new membranes; their performance and shrinkage temperature profile data are plotted in Figure 8 along with the corresponding data (solid lines) for the Batch 301 membranes which belong to the group II membranes referred above (Fig. 3 in our earlier report<sup>1</sup>). The results show that the performance and shrinkage temperature

profile data for the new membranes clearly lie in the region of the group II membranes, and the performance data in particular are very close to those of Batch 301 membranes. Again referring to Figure 7, the points *C* and *D* correspond to the solution temperatures used for the Batch 301 membranes (in group II) and the new membranes, respectively. Thus, if one wants to work at solution temperatures higher than 0°C and still obtain essentially

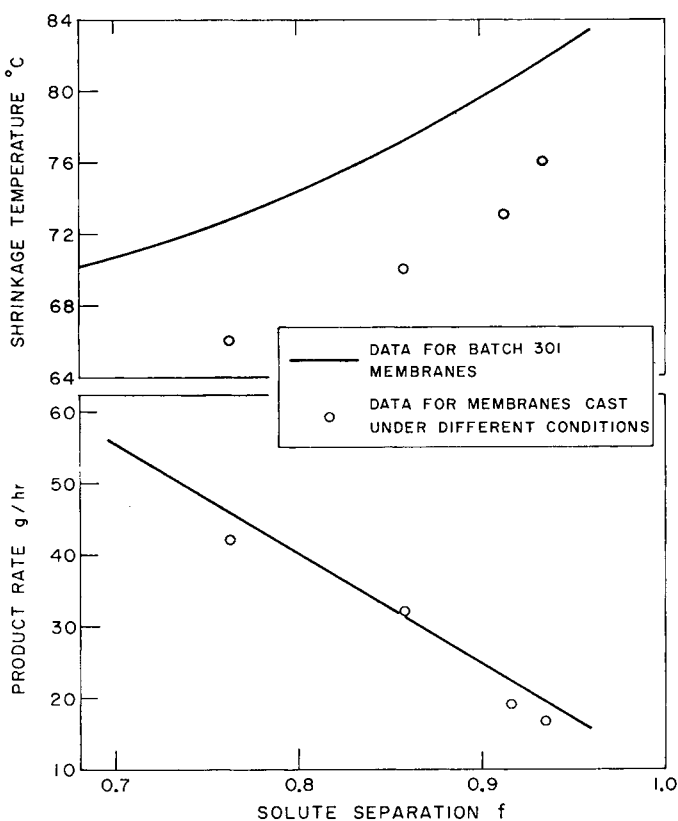


Fig. 8. Comparison of data on membrane performance and shrinkage temperature profile for membranes cast under different conditions with those of Batch 301 membranes. Casting solution composition (wt %): cellulose acetate, 17.4; acetone, 67.2; magnesium perchlorate, 1.52; water, 13.88; casting solution temperature, 24°C; casting atmosphere, ambient air at 24°C in contact with 30% acetone solution; evaporation time, 2 min. Reverse osmosis data for conditions: feed, 3500 ppm NaCl-H<sub>2</sub>O; operating pressure, 250 psig; mass transfer coefficient,  $45 \times 10^{-4}$  cm/sec; membrane area, 7.6 cm<sup>2</sup>.

the same membrane performance, one has to change the solution composition in the direction *AA'*.

These observations seem significant. They probably indicate that the structure of the solution of composition *A* at 0°C is comparable to the structure of the solution of composition *A'* at 24°C, and the remoteness of the phase boundary curves from any point representing the composition of

the casting solution is a useful measure of the state of the solution at the temperature corresponding to the boundary curve.

### CONCLUSIONS

The experimental data presented here give a quantitative confirmation of the governing significance of the solution structure–evaporation rate concept relating to the mechanism of phase separation and pore formation in the surface layer during the process of making reverse osmosis membranes. This concept thus opens new possibilities in the development and quality control of more productive reverse osmosis membranes.

The authors are grateful to Lucien Pageau and A. G. Baxter for their valuable assistance in the progress of these investigations. One of the authors (B. K.) thanks the National Research Council of Canada for the award of a postdoctoral fellowship.

Issued as N. R. C. No. 11523.

### References

1. B. Kunst and S. Sourirajan, *J. Appl. Polym. Sci.*, **14**, 723 (1970).
2. B. Kunst and S. Sourirajan, *Desalination*, **8**, 139 (1970).
3. P. Howard and R. S. Parikh, *J. Polym. Sci. A-1*, **6**, 537 (1968).
4. V. I. Klenin and N. K. Kolnibolotchuk, *Mekh. Protseessov Plenkoobrazov. Polim. Rastvorov Dispersii, Akad. Nauk SSSR, Sb. Statei*, **32** (1966).
5. V. I. Klenin and O. V. Klenina, *Mekh. Protseessov Plenkoobrazov. Polim. Rastvorov Dispersii, Akad. Nauk SSSR, Sb. Statei*, **45** (1966).

Received May 8, 1970

Revised May 20, 1970